Rifting a crustal mosaic – The influence of basement rheology and lithology on rift physiography in the Great South Basin, New Zealand

Thomas B. Phillips* & Ken J. W. McCaffrey

Department of Earth Science, Durham University, Science Labs, Elvet Hill, Durham, UK, DH13LE

*tbphil13@gmail.com

Abstract

The make-up of continental crust reflects its past tectonic history, containing a multitude of different lithological units and pre-existing structures that vary in strength with crustal properties typically varying across short distances. These variations exist across a range of scales and exert a great control over multiple aspects of rift physiography, including rift structural style, fault spacing and density, and the geometry of individual faults. We examine rift physiography across the Great South Basin, New Zealand, and show how variations in upper crustal lithology between basement terranes and the abundance and nature of pre-existing structures within these distinct areas influences the rift structural style from the rift to individual fault scale. We first characterise basement terranes beneath the Great South Basin, such as the sedimentary Murihiku Terrane or the dominantly granitic Median Batholith, and assess the pre-existing structures present within each. Secondly, we quantitatively analyse how extension was accommodated within each of these terranes by examining the structural style and calculating the fault density and beta-factor across a series of transects. In addition, we also examine fault behaviour at the boundaries between terranes, and the role of homogeneous granitic bodies in resisting extension and 'anchoring' sections of the rift. We compare the results of our study to examples from recently-published numerical modelling. However, we also highlight how local, small-scale complexities within rift systems can influence rift geometry at a scale below that typically analysed in modelling studies, emphasising the need for multi-scale analysis.

1 Introduction

Continental crust is a lithological and rheological smorgasbord comprised of a range of magmatic, sedimentary and metamorphic units, such as batholiths, metamorphic terranes and continental slivers, and sedimentary sequences, assembled and subsequently deformed through multiple tectonic events (e.g. Wilson, 1966; Thomas, 2006; McWilliams and Howell, 1982; Mortimer et al. 2004). Accordingly, these crustal units contain a multitude of pre-existing heterogeneities imparted through their unique tectonic history, both prior to and after being incorporated into their current crustal configuration. Such heterogeneities may include pre-existing fault systems and detachment surfaces within sedimentary sequences (Henza et al., 2011; Whipp et al., 2014), or ductile shear zones and prominent foliations within metamorphic units (Phillips et al., 2016; Heilman et al., 2019). These rheologically weaker units (i.e. sedimentary sequences), or those areas containing pervasive and well-developed heterogeneities, may preferentially localise strain, as evidenced by rotations in the local stress field surrounding shear zones or the exploitation of prominent fabrics by later faulting (Heilman et al., 2019; Philippon et al., 2015; Rotevatn et al., 2018; Samsu et al., 2021, 2022). In contrast, relatively undeformed areas of crust may include structures such as batholiths, which may be relatively pristine and contain few heterogeneities (Howell et al., 2020). These strong areas may cause strain to localise in adjacent, relatively weaker, areas as documented in analogue and numerical modelling (Beniest et al., 2018; Phillips et al., 2023; Samsu et al., 2021) or from observations of breakup along the Eastern North American margin (Lang et al., 2020). However, heterogeneities within these apparently stronger areas may also localise strain (e.g. Mair and Green 1981). As might be expected, each distinct unit within the continental crust manifests strain differently when subject to extension, and thus exerts some influence over the physiography of the incipient rift. These variations in crustal properties exist across a range of scales (e.g. Kirkpatrick et al., 2013), understanding their behaviour when subject to deformation is vital to understanding multiple aspects of rift evolution, from fault growth to seismic hazard assessments; these features typically fall below the resolution offered by crustal-scale seismic or numerical modelling studies.

Along with the bulk properties of each domain and the domain-specific heterogeneities, the boundaries between different crustal units also represent heterogeneities, either as discrete structures or prominent contrasts in rheological and lithological properties. These boundaries may represent areas of relative weakness, even between two stronger bodies, such as the formation of the Oslo rift between juxtaposed areas of cratonic lithosphere (Pascal and Cloetingh, 2002).

The orientation of the applied stress field and its relation to the crustal units and the boundaries between them is a key factor in how variable crustal properties influence rift development. If extension is oriented perpendicular to the boundaries between terranes, strain may localise in weaker areas whilst strong regions resist (e.g. Beniest et al., 2020; Lang et al., 2021; Samsu et al., 2022); however, if oriented parallel to the boundaries, each domain likely undergoes some strain, producing distinct and characteristic structural styles (Wright et al., 2020; Phillips et al., 2022). Furthermore, boundaries between units have the propensity to: i) directly reactivate, ii) segment and partition rift systems, or alternatively, iii) remain passive, depending on their orientation with respect to the applied stress field (Dore et al., 1997; Moy and Imber, 2009; Phillips and McCaffrey, 2019; Vasconcelos et al., 2019; Samsu et al., 2022).

This crustal mosaic of areas of laterally variable rheological and lithological properties, and changing proportions and types of pre-existing structural heterogeneities forms the substrate to developing rift systems, strongly influencing their geometry, structural style and evolution. In this study, we explore how this variable substrate influences rift physiography, the mechanisms by which they may do so, and establish characteristic structural styles associated with areas of relatively ‘strong’ and ‘weak’ crust. We use borehole-constrained 2D and 3D seismic reflection data to analyse the geometry and evolution of the Great South Basin (GSB), New Zealand to understand the role of the underlying crustal substrate on basin formation. The GSB formed atop and traverses a highly heterogeneous basement comprised of a variety of different basement terranes, including granitic batholiths and sedimentary sequences (Mortimer et al., 2004; Tulloch et al., 2019). We first examine the first-order rift geometry and establish the offshore continuations of the terrane boundaries identified onshore, before characterising the basement and rift structural style in each area using quantitative

measurements of fault spacing, heave and throw across key rift transects. We find that rift physiography varies markedly across the GSB, with characteristic structural styles associated with apparently ‘strong’ and ‘weak’ basement lithologies as well as the boundaries between them. We also document how localised and domain-specific features that are not often accounted for in modelling studies, such as self-contained, thin-skinned fault systems and localised basement highs, influence aspects of rift physiography across different scales. This complexity will be inherent to all natural rift systems and becomes significant when considering natural hazard or geoenergy applications in rift systems.

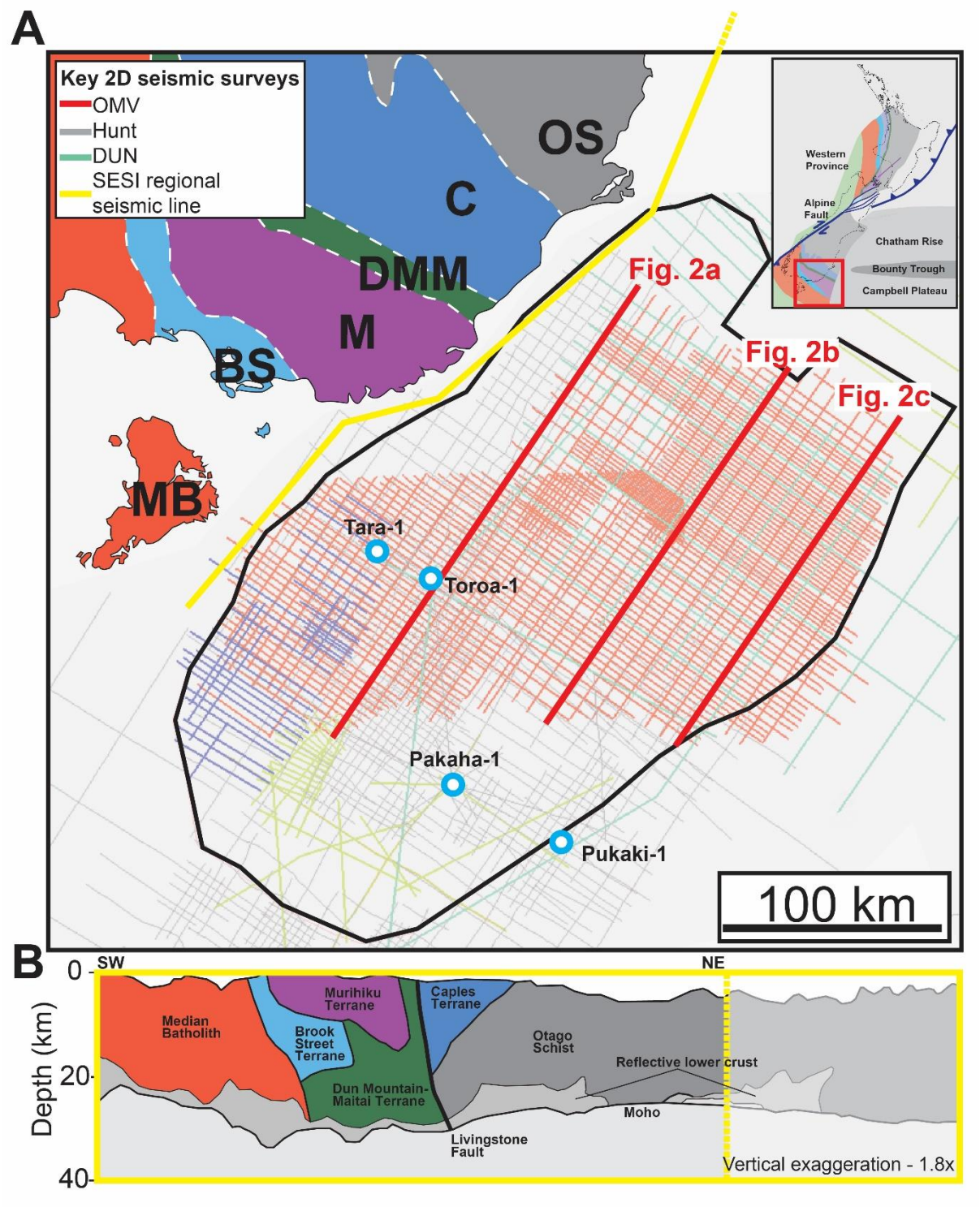

Figure 1 – A) Map showing the location of the study area and the onshore basement terranes of New Zealand's South Island. MB – Median Batholith; BS – Brook Street terrane; M – Murihiku terrane; DMM – Dun Mountain-Maitai terrane; C – Caples terrane; OS – Otago Schist. The wells and seismic data used throughout this study are also shown, with key, regional datasets labelled in the key (inset). B) Regional cross-section highlighting the crustal geology offshore the South Island of NZ. Based on the SESI seismic profile, after Mortimer et al., 2002. Light grey colours at the base of the crust represent areas of reflective lower crust. Whited out area to the northeast indicates where the section extends out of the area shown in 1a.

2 Geological Setting

2.1 Geological Setting

This study focuses on the Great South Basin, a NW-SE oriented rift system located off the eastern coast of the South Island of New Zealand (Beggs, 1993; Sahoo et al., 2014, 2020; Tulloch et al., 2019) (Figure 1). The basin is situated within the Campbell Plateau, a submerged area of thinned (22-32 km) continental crust, and is located to the south of the Bounty Trough, the Chatham Rise (Grobys et al., 2009; Mortimer et al., 2002) and the Canterbury Basin (Barrier et al., 2019) (Figure 1).

2.2 Basement geology

The basement geology of Zealandia comprises terranes that either formed part of Gondwana, or accreted along its southern margin during long-lived subduction from the Cambrian-Early Cretaceous periods (Bishop et al., 1985; Bradshaw, 1989; Mortimer et al., 2014). Collectively, these terranes are referred to as the Austral Superprovince, and can be divided into Eastern and Western provinces, separated by the Median Batholith (Mortimer et al., 2014). Basement terranes across New Zealand are offset along the Alpine Fault, such that those present in the South Island and beneath the GSB are also present off the western coast of the North Island beneath the Taranaki Basin (e.g. Muir et al., 2000; Collanega et al., 2019) (Figure 1).

The Great South Basin is underlain by Eastern Province terranes and the Median Batholith. Western province terranes are located to the southwest of the area, with the boundary between the southern margin of the Median Batholith and Western Province forming a reactivated terrane boundary (Phillips and McCaffrey, 2019). From south to north, the terranes beneath the GSB, based on limited well information and offshore projections, are: i) the Median Batholith, a long-lived cordilleran-style magmatic arc containing rocks of Carboniferous-Early Cretaceous in age (Mortimer et al., 1999); ii) the Brook Street terrane, a Permian-aged intra-oceanic arc system comprising volcaniclastic material (e.g. Robertson and Palamakumbura, 2019; Spandler et al., 2005); iii) the Murihiku Terrane, a relict fore-arc basin consisting of a thick Triassic-Early Cretaceous-aged sedimentary interval (Kamp and

Lidell, 2000; Campbell, 2019; Tulloch et al., 2019); iv) the Dun Mountain-Maitai (DMM) terrane, consisting of the Early Permian Dun Mountain ophiolitic sequence and later-derived sedimentary Maitai group (Kimbrough et al., 1992), bound to the north by the Livingstone Fault (Jugum et al., 2019; Robertson and Palamakumbura, 2019), and v) the Caples Terrane and Otago Schist, which become gradually more schistose to the north, outside of the study area (Bishop et al., 1976) (Figure 1).

2.3 Rifting in the Great South Basin

The main phase of extension in the Great South Basin occurred during the Late Cretaceous in response to the breakup of Gondwana (Barrier et al., 2019). Previous authors have suggested an earlier period of rift activity during the Jurassic, as evidenced by potential Jurassic strata in the Taranaki and Great South basins (Grobys et al., 2007; Uruski, 2010; Uruski et al., 2007). Extension in the Great South Basin is thought to have occurred via a two-stage process, initially associated with the breakup of Zealandia and Australia and the northwards propagation of the Tasman ridge (Kula et al., 2007; Tulloch et al., 2019). This was associated with activity along the Sisters Shear Zone to the south of Stewart Island (Kula et al., 2007, 2009). Subsequently, extension in the Tasman Sea halted and rift activity migrated to the south, associated with extension between Zealandia and Western Antarctica and the eventual formation of the Pacific-Antarctic ridge (Kula et al., 2009). This latter phase was associated with the main phase of rift activity in the Great South Basin (Sahoo et al., 2020) (Figure 2).

Oligo-Miocene subduction in the Tonga-Kermadec region, as well as the formation of the Alpine Fault placed New Zealand into a regional compressional regime (Bache et al., 2012; Cooper et al., 1987; Sutherland et al., 2000; Sutherland et al., 2010). Whilst the Great South Basin was relatively far-removed from this newly-formed plate boundary, compression was expressed as low-amplitude, long-wavelength folding across the area, leading to the development of the prominent Toroa anticline (Figure 2a).

Key stratigraphic intervals within the Great South Basin include Late Cretaceous syn-rift sandstones and prograding carbonate sequences throughout the Paleocene. At the Oligocene-Eocene boundary,

the Marshall Paraconformity forms a regional unconformity/paraconformity across the GSB, representing the onset of the Antarctic Circumpolar Current (Fulthorpe et al., 1996, Lever, 2007). At shallow depths, the GSB is characterised by a prominent prograding clinoform sequence.

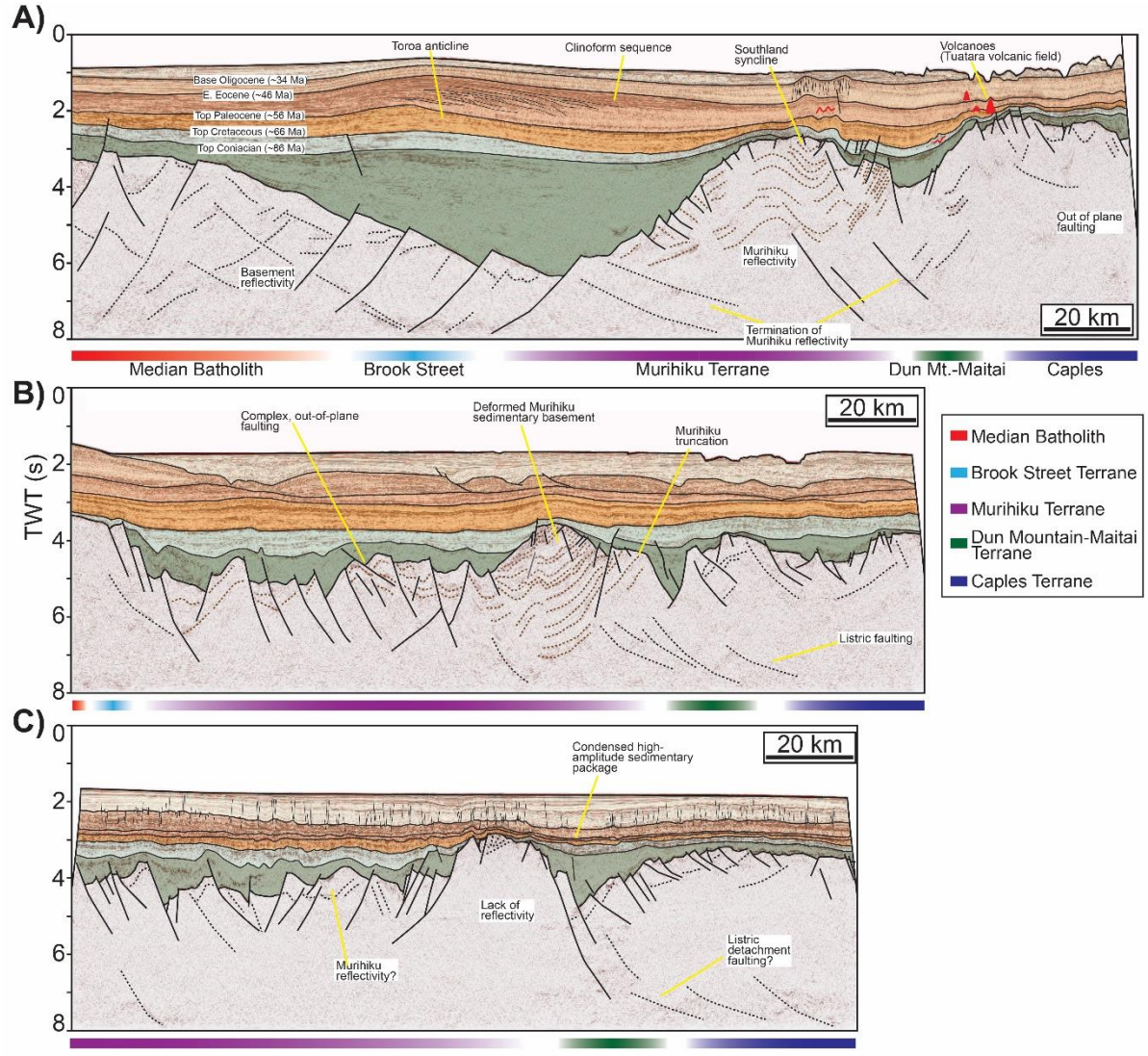

Figure 2 – Regional seismic sections running along-strike of the Great South Basin and traversing the different basement terranes. Offshore projections of the corresponding basement terrane is shown at the base of the section. Note how rift physiography changes between terranes and how the boundaries are often associated with fault systems, See figure 1 for section locations.

3 Data and Methods

3.1 Data

In this study, we analyse multiple 2D seismic datasets covering the Great South Basin, New Zealand. We primarily focus on the OMV 2D seismic dataset, which has a good spatial coverage over the majority of the GSB and also allows us to compare quantitative measurements and interpretations between sections with consistent acquisition and processing parameters. In addition to this, we also use additional seismic surveys, including the Hunt and DUN 2D seismic surveys, which fill in gaps not covered by the OMV survey (Figure 1a). Image quality within the Hunt survey is lower than that of the OMV survey, whilst the DUN survey has a much greater spacing between individual sections. Seismic data are presented as zero-phase and follow the SEG normal polarity convention; a downward increase in acoustic impedance, such as the seabed, is represented by a peak, and a downwards decrease by a trough.

3.2 Seismic interpretation

We interpret 7 seismic horizons across the area, including the seabed. Complete coverage is provided across the GSB for the top basement surface (Figure 3a), whilst the Top Cretaceous horizon is also mapped across the majority of the area (Figure 3b). Additional horizons are interpreted where possible and across individual sections. We mapped prominent seismic reflections and tied them to stratigraphic formations as defined in four wells across the GSB (Figure 1a). These boreholes provide good constraints on horizons, including basement, across the area, and in some cases provide spot-constraints on which basement terranes is present at depth. The mapped horizons in the sedimentary cover correspond to: i) Top basement; ii) Top Coniacian (~66 Ma); iii) Top Cretaceous (~60 Ma); iv) Top Paleocene (~56 Ma); v) Early Eocene (~46 Ma); vi) the Base Oligocene Marshall Paraconformity; and vii) the seabed (Phillips and McCaffrey, 2019; Sahoo et al., 2020, Phillips and Magee, 2020).

Good data quality across the majority of the area gave a high degree of confidence to the interpretations, however, due to the large distances between wells some discrepancies and variation

may be present. Furthermore, post-rift horizons often proved difficult to prove across the east of the area due to a lack of well coverage and the condensed nature of the stratigraphic succession in this interval. Although, the exact reflections were often difficult to follow in this area, the overall package could be mapped with relative confidence. The top basement surface proved difficult to map in certain areas. In some locations the top basement surface was buried to great depths, reducing confidence in the interpretation, whereas in areas of the Murihiku terrane, the distinction between syn-rift strata and the sedimentary basement was hard to identify. In the latter case, we based the top basement interpretation on truncations of the basement strata. Although some interpretations of the depth of top basement surface were relatively low confidence, we are able to identify faults cutting the top basement horizon with relatively high confidence.

3.3 Quantitative fault analyses

We measured key fault properties (i.e. spacing, heave) along transects corresponding to the Median Batholith, Murihiku and DMM/Caples terranes in order to analyse how the structural style and physiography of the rift changed along-strike between basement terranes (see Figure 3 for transect locations). In addition, we undertook quantitative analyses of individual faults, in the form of throw-length plots, to understand their geometry and evolution, particularly in relation to the boundaries between different terranes.

We calculated the number of major faults, average fault spacing, heave and the beta factor for each transect. We only measured major fault systems across each section (> 0.5 s TWT displacement) and discounted low-displacement structures for the purposes of these analyses. Faults that join together at depth or are closely spaced are interpreted as belonging to the same system. A maximum transect length representing that of the whole transect, including any rift margins was measured, whereas a minimum value was defined from a point at the hangingwall/footwall of the initial and final faults along the transect. One caveat with our transect-based approach is that the Median Batholith transect is from a different survey than the others and is formed of multiple sections that do not follow a direct

straight line; accordingly, we only draw first-order comparisons and correlations between different transects.

We used throw-length plots to analyse the geometry of individual faults proximal to the terrane boundaries. Throw was calculated between hangingwall and footwall cutoffs of the Top Basement horizons. Throw-length analyses record both brittle (fault-related) and ductile (fold-related) components of deformation, therefore, in areas of near-fault, fault-parallel folding, we project the horizon towards the fault using the regional (i.e. unaffected by fault-related folding) dip of the horizon away from the fault. Measuring this value incorporates both the brittle and ductile components of deformation. The measurements for each fault were centred on a seismic section that roughly corresponded to the terrane boundary, allowing faults to be projected onto the same line and for comparison between individual faults. A wider tolerance around this section was also included to account for variation and uncertainty in the exact location of the terrane boundary.

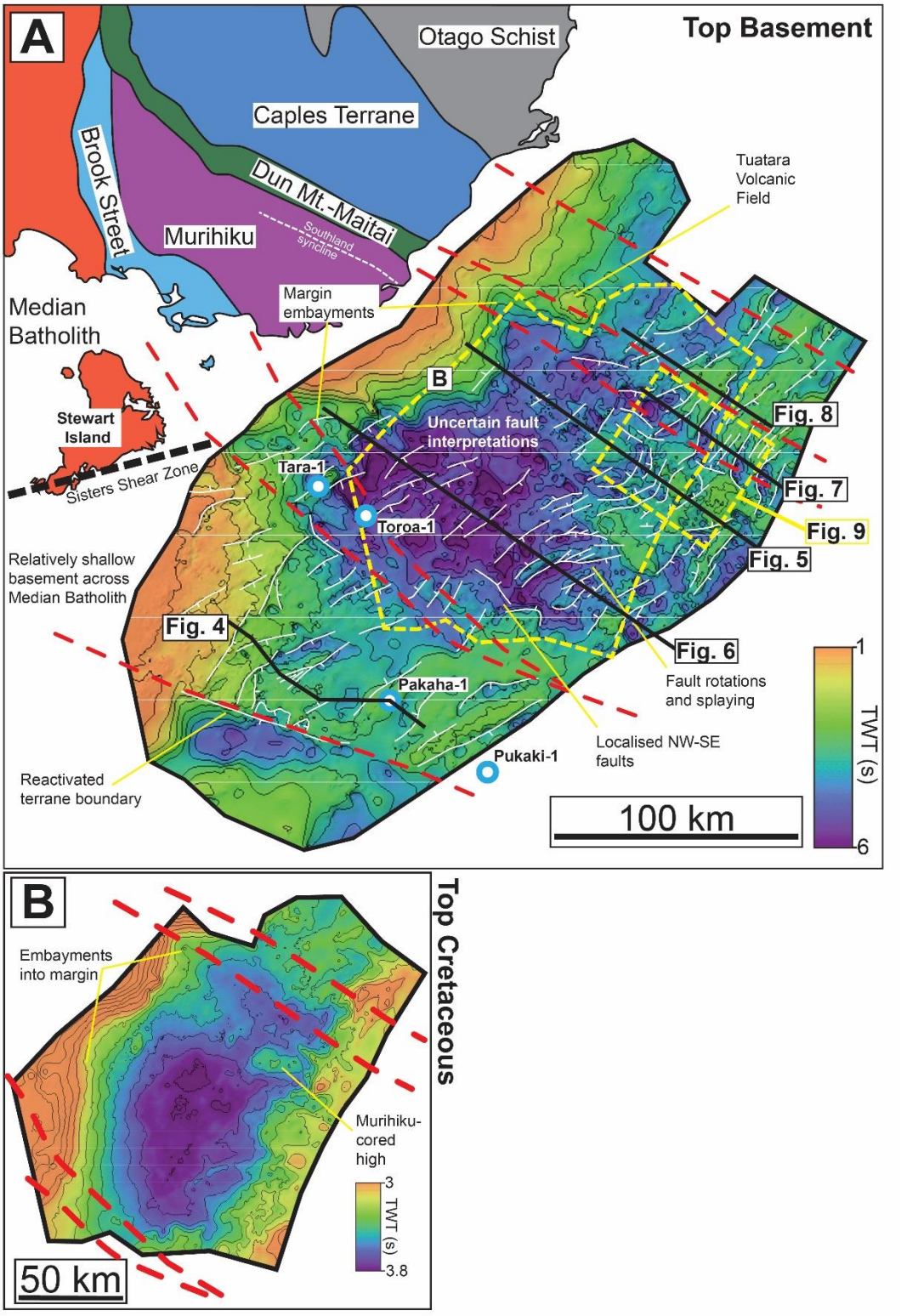

Figure 3 – A) TWT structure map of the top basement surface across the Great South Basin. The offshore extensions of the onshore terrane boundaries are shown after Ghisetti (2010) and Mortimer et al., (2002). Figures 4, 5, 6, 7 correspond to transects across the Median Batholith, Murihiku terrane (North), Murihiku terrane (South), Dun Mountain-Maitai terrane, and the Caples terrane, respectively. B) TWT structure map of the Top Cretaceous surface across the centre of the study area with terrane boundary projections overlaid. See Figure 3a for location.

4 Rift physiography

Rift physiography and structural style in the Great South Basin changes markedly along-strike (Figure 3). Basement terranes are clearly defined onshore and can be traced short distances offshore through regional seismic sections (Mortimer et al., 2002). Local constraints on the basement geology beneath the rift can be found via four basement-penetrating boreholes (Figure 3a), the Pakaha-1 and Pukaki-1 boreholes penetrate basement corresponding to the Median Batholith. Based on the regional configuration of the terranes onshore we do not expect any major deviations in the geometries of the boundaries offshore, hence the projected boundaries are approximate.

Additional lines of evidence can be used to project the extension of the terrane boundaries offshore. The SESI deep seismic line provides near shore constraints on the offshore extension of the basement terranes (Mortimer et al., 2002). The boundary between the DMM and Caples terranes is represented by the Livingstone Fault onshore, a 100's of m-to-km wide shear zone onshore (Figure 1b) (Tarling et al., 2019), that has previously been proposed to act as a conduit for the Tuatara volcanic field magmatism offshore in the Great South Basin and beneath the North Island (Phillips and Magee, 2020; Hopkins et al., 2020). In addition, the ophiolitic DMM terrane is associated with the prominent negative Junction magnetic anomaly that can be traced some distance offshore (Sutherland et al., 2000; Phillips and Magee, 2020). Similarly, the southern boundary of the Median Batholith has previously been identified as a reactivated crustal-scale shear zone (Phillips and McCaffrey, 2019). Further studies have also identified areas where faults rotate and terminate at the offshore continuations of terrane boundaries (Sahoo et al., 2020).

Along with the offshore continuations of their boundaries, the Murihiku terrane is also associated with a characteristic basement seismic facies; it is often easy to identify due to its sedimentary nature producing a layered basement reflectivity (Tulloch et al., 2019). This layered basement facies can be distinguished from the overlying syn-rift strata based on truncated stratigraphic relationships at the top basement surface. The characteristic Murihiku basement facies becomes difficult to identify to the southwest where the rift is deeper and basement is buried to greater depths (Figure 2, 3).

The deepest section of the basin, reaching ~7 s TWT, is located in the offshore extension of the Murihiku and Brook Street terranes (Figure 3). The basin displays a uniformly shallower depth to the south across the Median Batholith (~3-4 s TWT), and also further to the north across the Caples terrane (~4 s TWT) (Figure 3). Two embayments are identified along the western rift margin. These are ~20-30 km wide and ~10-20 km deep, corresponding to the offshore extensions of the Brook Street and DMM terranes. The former may in part relate to the offshore extension of the Sisters Shear Zone, located to the south of Stewart Island (Figure 3a) (Kula et al., 2009). We also observe that the basin, along with the top basement surface, shallows outboard to the east, regardless of the basement terrane.

We interpret that the Median Batholith underlies the shallow rift section to the southwest; its southern boundary is represented by a crustal-scale shear zone (Phillips and McCaffrey, 2019), and its northern boundary with the Brook Street terrane strikes NW-SE and delineates the southern margin of the deeper rift section. The rift deepens northwards across the Brook Street terrane, where some faults appear to step down to the north, which we suggest represents the boundary between the Brook Street and Murihiku terranes. The Brook Street terrane is purported to taper and terminate to the southeast, such that the Murihiku terrane is juxtaposed directly against the Median Batholith. Although Murihiku basement is associated with a characteristic seismic expression, this is difficult to identify to the south and as such, the southern margin of the Murihiku terrane is difficult to accurately constrain. To the north, the boundary between the Murihiku and DMM terranes is identified based on a change in the basement seismic character, and the termination and change in polarity of fault systems. This boundary also appears to be associated with a series of NE-dipping faults at 6-8 s TWT depth on seismic data. These faults may represent the expression of the boundary, or the terrane bounding fault, within the middle-to-lower crust (Figure 2).

The basement terranes and associated basin segmentation can also be identified at shallower stratigraphic depths (Figure 3b). The main depressions identified on the top Cretaceous surface correspond to the distribution of depocentres across the top basement surface (Figure 3). The deepest

part of the basin sits atop the Murihiku terrane subcrop on the top Basement surface. A further depression is present to the north, above that overlying the DMM terrane.

5 Domain specific rift structural style

Having described the overall structure of the GSB and constrained the offshore continuations of the terrane boundaries beneath it (Figure 3), we now characterise key structural styles associated with each of the different terranes. For the Median Batholith, Murihiku Terrane and the DMM/Caples terranes, we describe the basement seismic character and fault systems, and report average fault spacing, throw and heave along each of the transects.

5.1 Median Batholith – Granitic basement

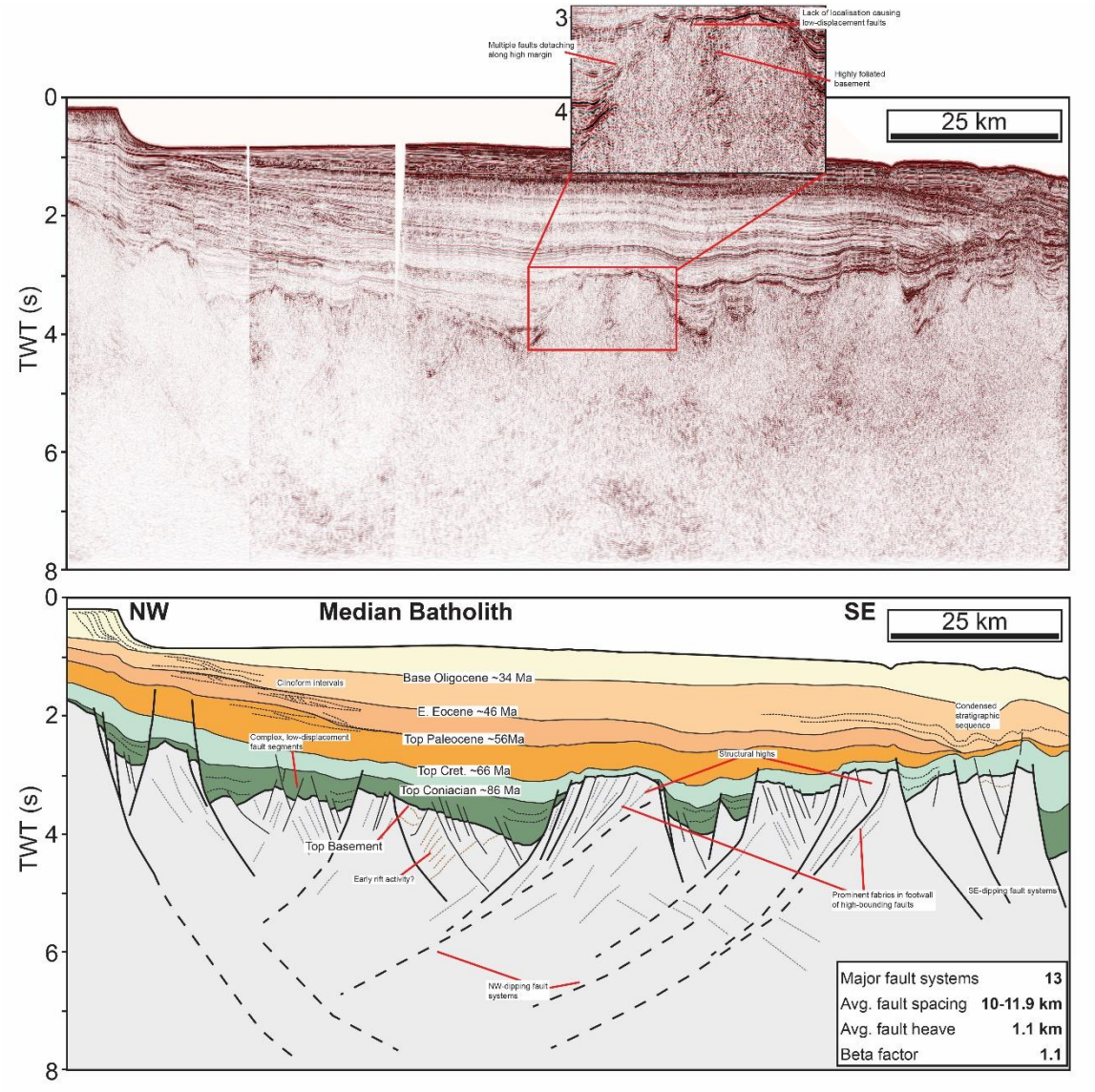

Figure 4 – Uninterpreted and interpreted seismic section showcasing the rift structural style across the Median Batholith. See Figure 3a for location. Note the presence of large, linked NW-dipping fault systems and multiple basement highs. Inset – Close-up uninterpreted section of one of the basement highs, showing multiple faults detaching along the margin of the structure and merging together at depth.

The Median Batholith underlies the shallowest section of the rift, with the deepest point reaching ~4 s TWT. It is dominated by numerous relatively low-displacement faults (0.1-0.2 s TWT throw), with a number of infrequent high-displacement faults (~1 s TWT throw) also present. The high-displacement faults typically bound basement highs, with two major highs identified in the centre and towards the SE of the transect (Figure 4). The high-displacement fault systems generally comprise multiple fault

segments that dip in the same direction and merge together at depth. Low-displacement, closely-spaced faults are present across the section, interspersed between these larger structures. We identified 13 major fault systems along the transect, with an average spacing of 10.9-11.9 km. The average heave per fault system was ~1.1 km, giving a beta factor along the transect of ~1.1 (Figure 4). Further extension is likely accommodated by the smaller displacement faults, although these are not incorporated into the transect results.

Aside from the SE-dipping rift-bounding fault at the NW end of the transect, the majority of faults in this area dip to the NW, with some SE-dipping faults present to the SE of the transect. A series of conjugate SE- and NW-dipping faults, displaying complex cross-cutting relationships are present towards the NW part of the section. These correspond to the 'Splaying Fault System' described by Phillips and McCaffrey (2019), where a single fault splays and terminates towards the boundary with the relatively strong Separation Point Batholith suite within the composite Median Batholith.

Basement reflectivity is highly variable across the section, although this may be partially related to the transect comprising sections from different seismic surveys, each with different acquisition and processing parameters. This notwithstanding, some prominent reflectivity is present beneath the top basement surface and can be correlated across different survey sections. We identify local areas of layered reflectivity immediately below the top Basement surface that we interpret as sedimentary layering, perhaps representing an earlier phase of activity. In addition, some deeper reflectivity appears to represent the continuation of rift-related faults. These deeper structures are most commonly associated with the basement-high bounding faults. Elsewhere along the transect, some areas are characterised by prominent fault-parallel fabrics that are not associated with any offset of the top basement surface. These fabrics are often located in the hangingwall of major fault systems, we suggest that the fabrics correspond to prominent foliation within basement that may represent faults displaying typical displacements that are below seismic resolution.

Cretaceous strata, particularly pre-Coniacian (>86 Ma), form the syn-rift stratigraphic interval across the transect. The post-rift stratigraphic sequence, particularly the Cretaceous-Early Eocene (66-46 Ma) interval becomes increasingly condensed towards the southeast, thinning from ~1000 to ~100 ms

TWT across the section. This condensed stratigraphic interval also corresponds to a relative basement high.

5.2 Murihiku Terrane – Sedimentary basement

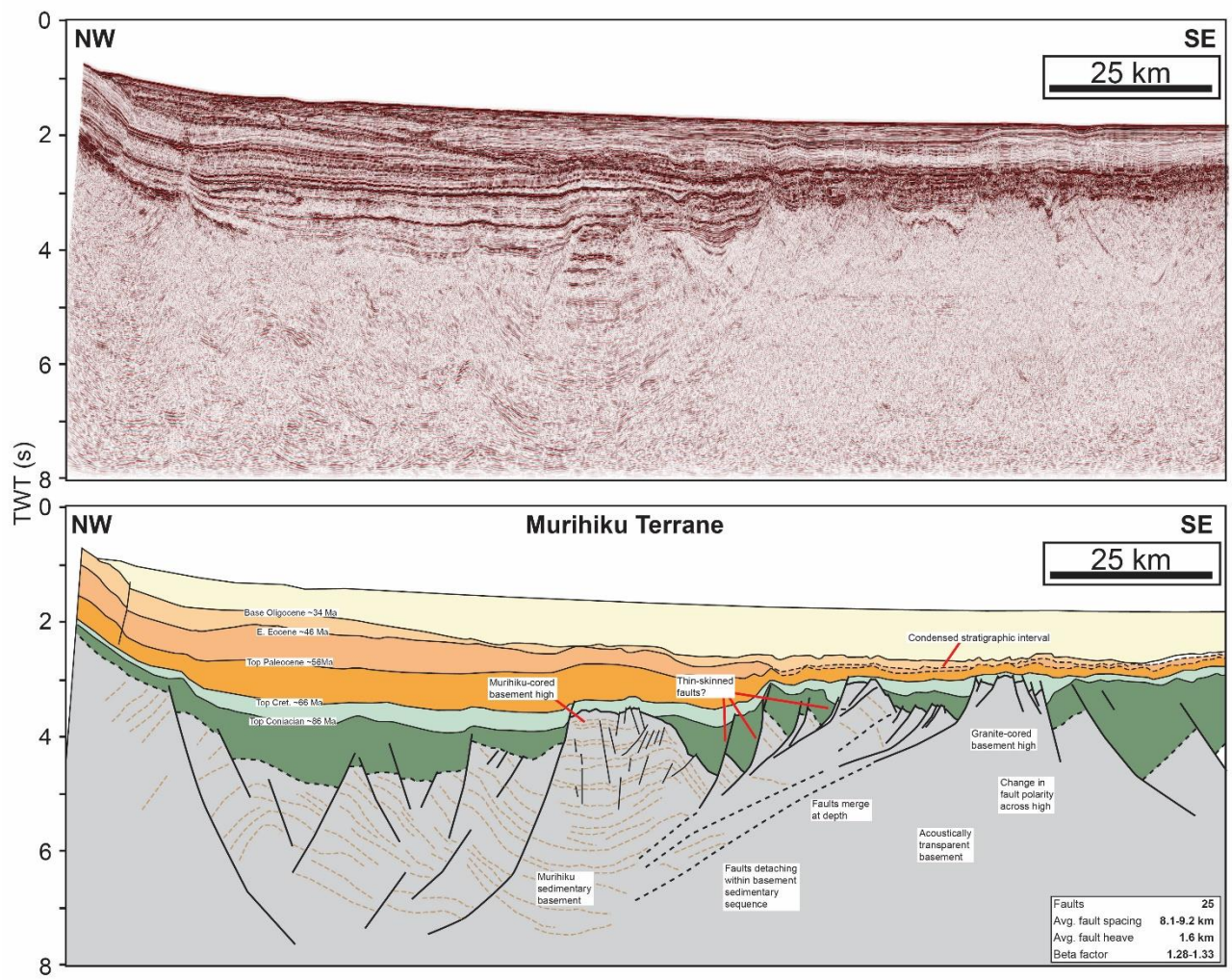

Figure 5 – Uninterpreted and interpreted seismic section showing the basement character and rift structure across the northern Murihiku Terrane. See Figure 3a for section location. Note the sedimentary layering within the basement and the relatively transparent basement associated with the granite-cored high.

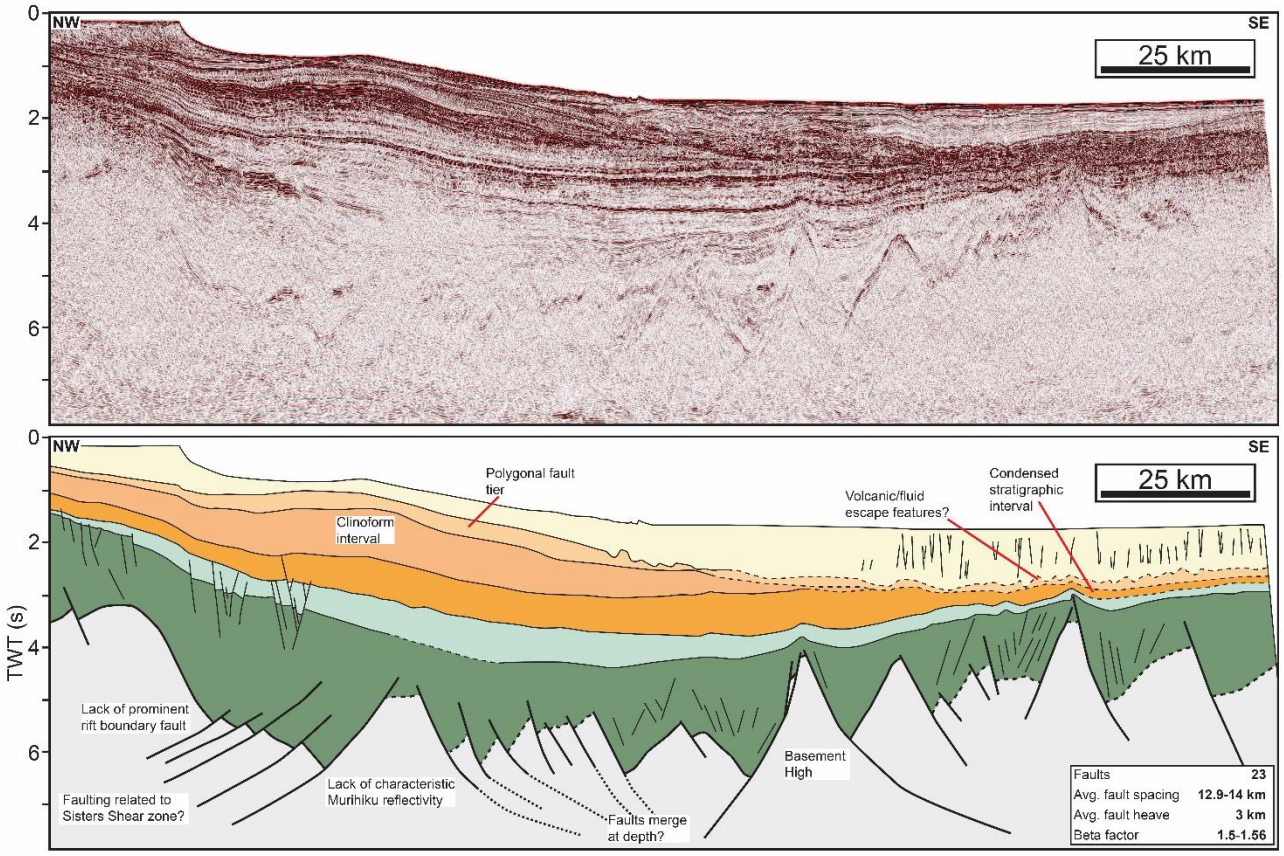

Figure 6 – Uninterpreted and interpreted seismic section showing the basement character and rift structure across the southern Murihiku Terrane. Note the narrow basement highs bound by closely spaced faults that may merge at depth.

Basement of the Murihiku terrane is easily identifiable by its diagnostic seismic expression. The sedimentary nature of the Murihiku Terrane gives rise to a distinctive highly reflective and layered expression on seismic reflection data (Figure 2, 5). Due to this distinctive seismic expression, well-developed folding can be identified within the basement. A series of faults are identified offsetting the basement reflectivity (Figure 5). Whilst some of these structures may relate to Late Cretaceous rifting in the Great South Basin, others likely represent relict structures formed prior to extension that may have subsequently been reactivated during the formation of the GSB. Prominent folding is also present within the Murihiku terrane offshore. One such syncline is interpreted as corresponding to the offshore extension of the Southland Syncline, a major structure also identified onshore (Figure 2, 3) (Tulloch et al., 2019). Further synformal and antiformal folds are also identified, although these are not specifically linked to onshore structures (Figure 5).

The characteristic layered seismic expression extends to ~7 s TWT depth, below which structure is difficult to resolve. The Top Basement surface is typically deeper than that of the Median Batholith, at

~5-6 s TWT (Figure 5, 6), with the terrane associated with the deepest section of the basin at ~6-7 s TWT (Figure 3, 6). Some uncertainty is associated with basement depth towards the south and west due to difficulties in distinguishing syn-rift and basement sedimentary strata, however, we remain confident in our interpretations based on correlations and continuation of the clear Murihiku Terrane further East (Figure 5).

Rift physiography across the northern part of the Murihiku terrane is characterised by relatively highly spaced (8.1-9.2 km), high-displacement (~1 s TWT) faults. Average fault heave is 1.6 km, with the section displaying a beta factor of 1.28-1.33 (Figure 5). The majority of faults across the section dip towards the NW, apart from the western boundary fault of the rift and those in the southeast of the transect. In the centre of the transect, a number of faults form part of a thin-skinned system that links together at depth and appears to detach within the Murihiku sedimentary basement (Figure 5). A major Murihiku-cored basement high is situated within the hangingwall of this thin-skinned fault system (Figure 5). In plan-view, the thin-skinned faults display a highly arcuate geometry, concave to the southeast, suggesting that the thin-skinned fault system has translated the Murihiku-cored high north-westwards (Figure 3a). A further basement high is present to the southeast, located in the footwall of the thin-skinned detachment system. Unlike the high to the west, this high does not show any Murihiku-type basement layering and instead appears relatively acoustically transparent (Figure 5). This high also marks a change in the dominant fault polarity across the transect, with NW-dipping faults present to the west and SE-dipping faults to the east. We interpret that this high represents a granite-cored basement high, similar to those identified in the Median Batholith. This ‘fixed’ basement high forms a backstop to the thin-skinned detachment fault systems that translated the Murihiku-cored high westwards.

The structural style of the Murihiku Terrane changes towards the south, as evidenced by the second transect (Figure 6). The characteristic layered basement reflectivity is no longer present, potentially due to being buried to greater depths (Figure 6). This section is characterised by 23 closely-spaced (12.9-14 km) faults that display an average heave of 3 km. The calculated beta factor across this section of the Murihiku terrane is larger than that to the north (1.5-1.56), with the basin reaching

greater depths (~6 s TWT). This second transect intersects a large depocentre in the west along with additional, predominantly SE-dipping faults to the east. The large depocentre displays a central high with NW- and SE-dipping fault systems to the NW and SE respectively. Each of these faults systems comprises multiple faults that appear to merge together at depth (Figure 6). A narrow basement ridge is present in the centre of the section; this ridge displays a curved geometry in plan-view, splaying towards the north (Figure 3a).

As across the Median Batholith, the post-rift stratigraphic sequence thins abruptly towards the east across both Murihiku terrane transects, with evidence of erosion and truncation present in some areas, although this is difficult to confirm (Figure 5, 6). The post-rift interval in the west of the area may be thickened by the presence of clinoform sequences sourced from the mainland, although these usually pinch out to the west of the area of abrupt thinning (Figure 6). A further point of note is that the Paleocene interval, which is predominantly not clinoform-bearing, also thins to the east. This transition from thick to thin post-rift succession occurs to the east of the Murihiku-cored basement high, atop the thin-skinned detachment system.

5.3 Dun Mountain-Maitai and Caples Terranes

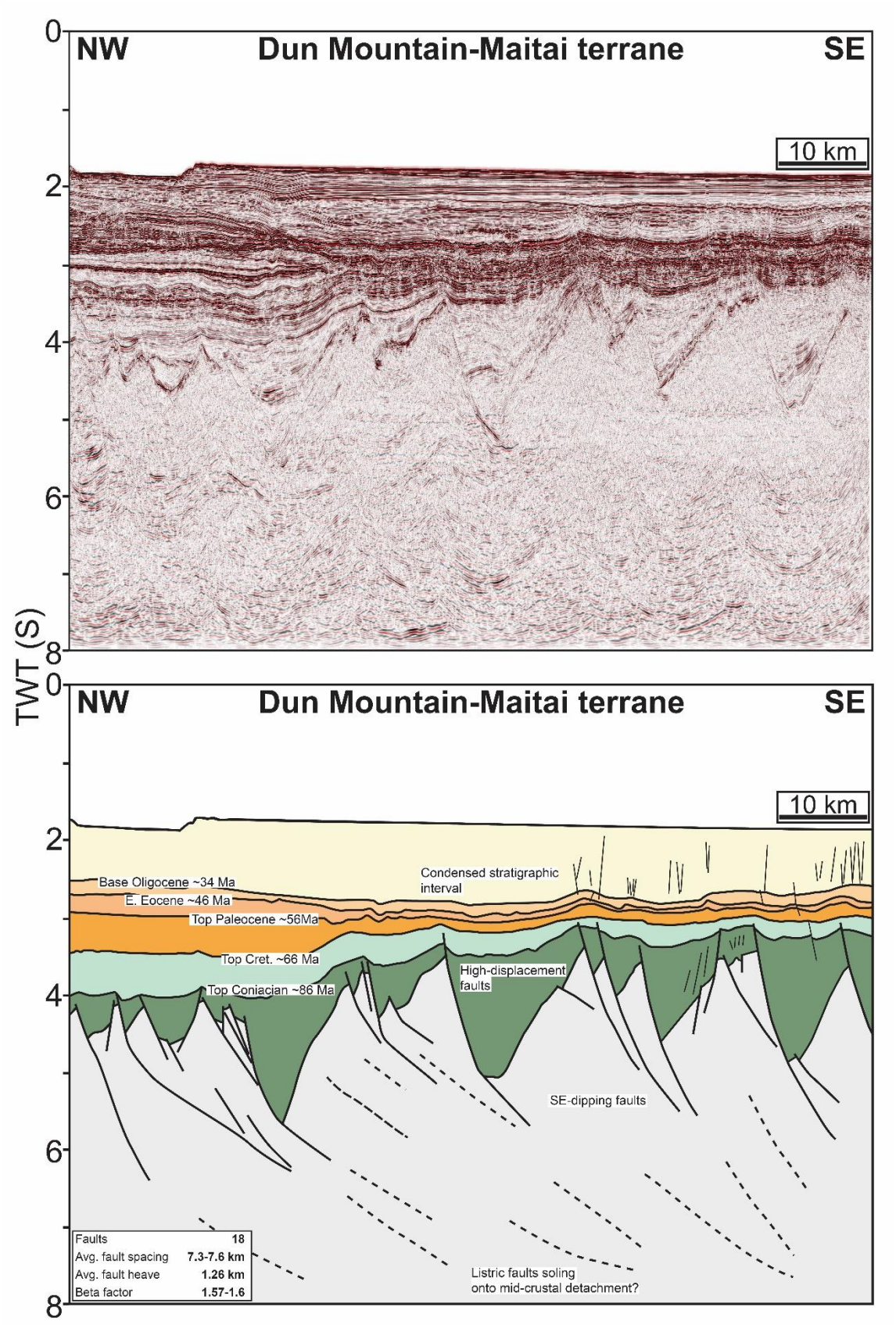

Figure 7 –.Uninterpreted and interpreted seismic section showing the basement character and rift structural style across the Dun Mountain-Maitai terrane. See Figure 3 for section location. Similar structural styles are identified beneath the adjacent Caples terrane. Note the dominant SE dip of the faults that appear to sole onto a potential mid-crustal detachment.

The DMM terrane is relatively narrow in plan-view (~20 km) and not fully parallel to the seismic sections, such that any transect likely traverses both it and the Caples Terrane to the northeast. As we see little variation in rift physiography in map-view between the two terranes (Figure 3a) we analyse the DMM and Caples terranes collectively. The Tuatara Volcanic Field dominates to the northwest of the terranes and obscures any rift-related faulting, deeper sedimentary horizons, and any basement structure. The siting of this volcanic field has been suggested to be controlled by the Livingstone Fault, which forms the boundary between the DMM and Caples terranes (Phillips and Magee, 2020).

The DMM/Caples transect (Figure 7) is characterised by 12 high-displacement (>1 s TWT, 18 faults in total), regularly spaced (7.3-7.6 km) fault systems that display a dominant southeast dip. These high-displacement faults produce large topographic variation in the depth of the top-basement surface across the transect, which is around 4-6 s TWT. The average heave for the fault systems is ~1.26 km, with the transect displaying a beta factor of 1.57-1.6. No characteristic basement seismic facies are identified along the transect, in contrast to the Murihiku terrane. Some basement reflectivity, which we relate to the continuations of the major faults, and potentially additional faults entirely within basement, is present at greater depths (Figure 7). The predominant southeast dip of faults along the transect and their apparent listric geometry, may suggest that they sole out at depth within the mid-crust. This is in agreement with previous authors who suggest that SE-dipping listric faults within the Great South Basin sole onto a mid-crustal detachment (Uruski et al., 2008), although this is not apparent across the Median Batholith and Murihiku terranes.

As also observed along the Median Batholith and Murihiku Terrane sections, the post-rift stratigraphic interval across the DMM and Caples terrane becomes condensed and thins towards the SE (Figure 7). The thinned post-rift succession identified here and along the southeastern margin of the Great South Basin (Figure 2c) appears to have been deposited in an area that had a lower amount of accommodation space present. Across this section, no change in the amount of syn-rift fault activity is identified, suggesting that this is not related to differential post-rift thermal subsidence.

5.4 Isolated basement highs

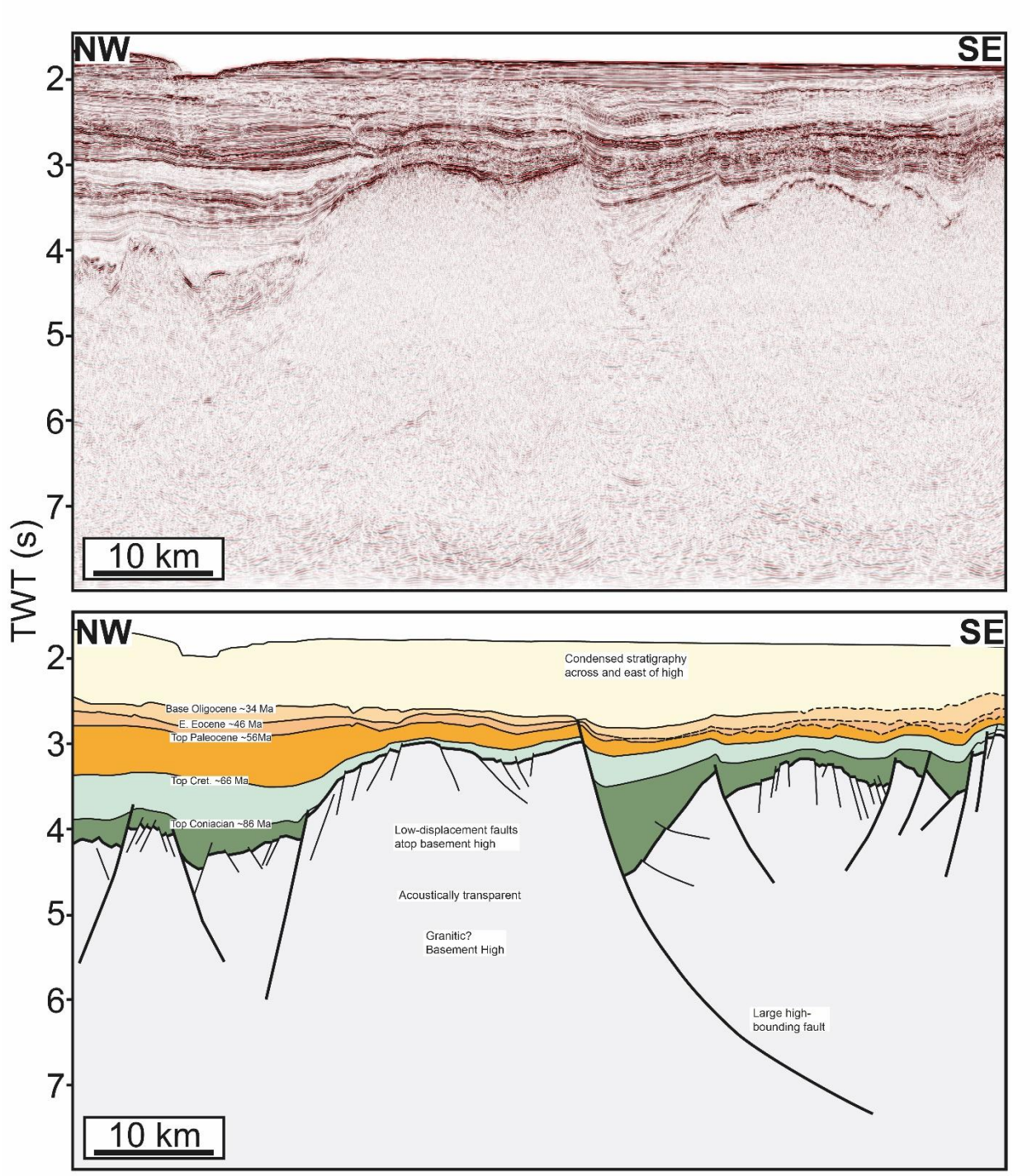

Figure 8 – Uninterpreted and interpreted seismic section showing the rift geometry across an isolated basement high. The high is bound by a large, listric fault with smaller-scale faults present within the crest of the basement high.

One commonality between the different terranes is the presence of basement highs, particularly towards the east where they are typically located beneath the thinned post-rift succession (Figure 5, 8). With the exception of the Murihiku-cored basement high, the highs are associated with a lack of

internal faulting, high-displacement faults along their margins and an acoustically transparent basement seismic character. They appear to represent isolated bodies within a range of different terranes.

Data from wells that penetrate the basement highs, together with their acoustically transparent seismic character (Figure 8), suggests they are granitic in composition (Tulloch et al., 2019; Omosanya et al., 2021). The highs are characterised by a lack of major faulting, with only minor faults present close to the top. They are often bound by high-displacement faults that extend to great depths, with additional smaller faults often present in the footwall of the bounding fault (Figure 8). In plan-view, multiple faults extend partway into the basement highs before terminating (Figure 3). In three-dimensions, we suggest that the faults do not extend far into the granite; rather, the faults rotate to shallower dips as they approach the granitic high. These faults are cross-cut by the large bounding fault (Figure 8).

6 Terrane boundaries

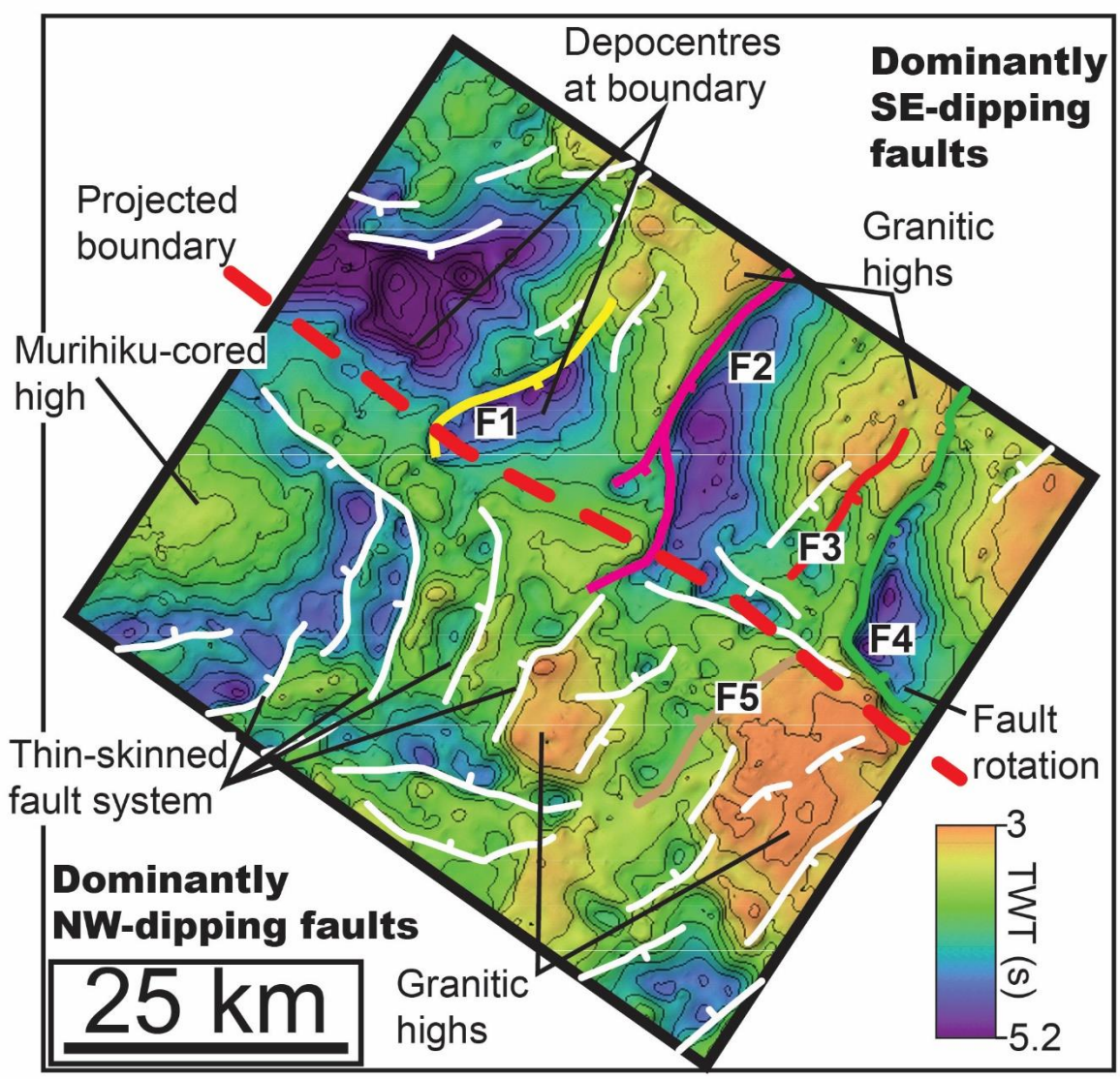

Figure 9 – Close up map showing the top basement surface in the area around the boundary between the Murihiku and DMM/Caples terranes. Note the change in fault polarity that occurs across the projected terrane boundary. Coloured faults represent those shown in Figure 10. See Figure 3 for location.

Along with the characteristic rift structural styles associated with each of the basement terranes and the basement highs, we also identify prominent changes in rift physiography and faulting at terrane boundaries. This appears to reflect the transition between the characteristic styles associated with each domain, but also an influence from the boundary itself as an active feature.

Some of the projected terrane boundaries correlate with the location of anomalously oriented NW-SE-oriented faults, such as between the Median Batholith and Brook Street terranes, and the Murihiku

and DMM terranes (Figure 3a), as well as the locations of major depocentres and basins. Faults can also be identified rotating and aligning along terrane boundaries (Figure 9), or they may splay and segment at the boundary, with only some segments extending into the adjacent terrane (Figure 9, 10).

Some features are identifiable across multiple sections and appear to represent the manifestation of a terrane boundary. A prominent example is the Murihiku-DMM boundary, which is associated with a series of SE-dipping faults at depth (Figure 2), these structures also mark the north-eastern termination of Murihiku reflective basement. The Murihiku-DMM terrane boundary is also associated with a change in fault polarity, from NW-dipping faults in the Murihiku terrane to the south and SE-dipping faults in the DMM terrane to the north (Figure 9). The NW-dipping faults within the Murihiku terrane form part of a self-contained, thin-skinned fault system that seems to detach onto horizons internally within the sedimentary basement of the terrane (Figure 5).

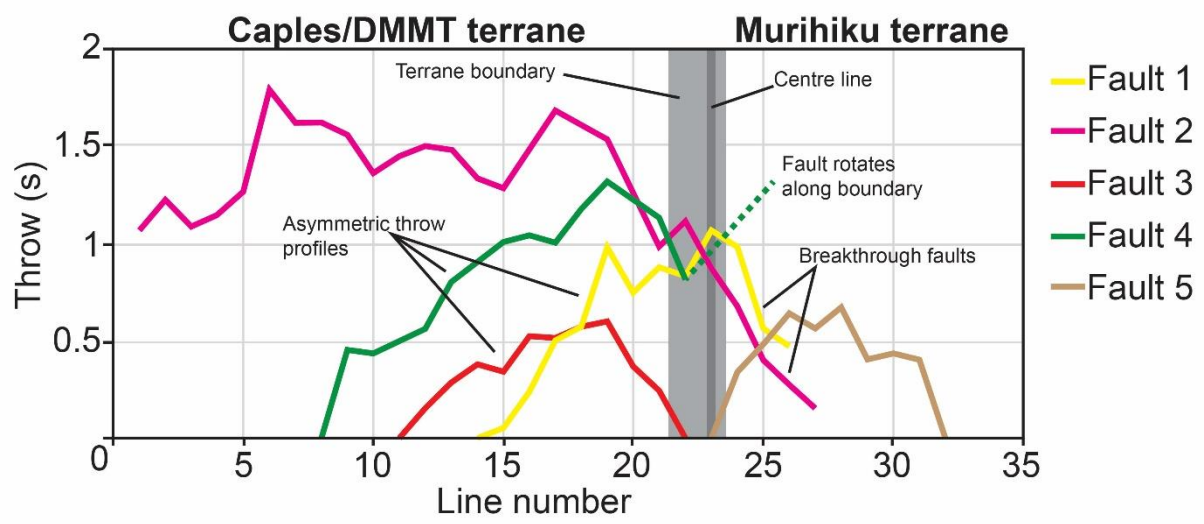

Figure 10 – Throw-Length plots across the top basement surface for faults proximal to the terrane boundary. See Figure 9 for map view fault geometry and location. The terrane boundary is indicated by a grey area whilst the centre line represents a seismic line where throw measurements were pinned for all faults. Measurements were then taken on adjacent lines moving away from this fixed point along-strike of the faults.

Along with the qualitative observations outlined above, we undertook a series of throw-length plots along faults within the DMM terrane and the Murihiku terrane. The majority of faults within the Murihiku terrane form part of a thin-skinned system rooting beneath the Murihiku-cored high (Figure 5). These faults typically rotate along the terrane boundary and are therefore not considered in our quantitative analyses. We analyse one fault within the Murihiku terrane towards the southeast (Fault

5, Figure 10); this fault bounds a granitic basement high and forms the backstop to the thin-skinned fault system (Figure 9). Faults within the Caples/DMM terranes display throw maxima at or close to the terrane boundary (Figure 10) . Fault 2 displays relatively high throw values along its length and continues further to the north (Figure 10). Faults 3 and 4 within the Caples/DMM terranes display throw maxima of ~0.6 s TWT and ~1.3 s TWT respectively, with these maxima located close to the projected terrane boundary. The throw maxima of Fault 1 (~1 s TWT) is located at the boundary. Each of these faults displays an asymmetric throw profile, skewed towards the terrane boundary. In contrast, Fault 5 located within the Murihiku terrane, displays a symmetric throw profile with a central throw maxima (~0.7 s TWT). Fault 3 terminates at the terrane boundary, whereas Fault 4 rotates to align with it. Both Fault 2 and Fault 3 appear to extend across the terrane boundary with relatively low throw values in the adjacent Murihiku Terrane. In the case of Fault 1, the fault terminates a short distance into the terrane, which may indicate that the fault is actually inhibited at the boundary and instead rotates along it (Figure 9). However, Fault 2, the largest fault, traverses and appears to show some segmentation at the boundary. This segmentation may reflect a period of initial retardation before the fault eventually propagated through the terrane boundary.

7 Discussion

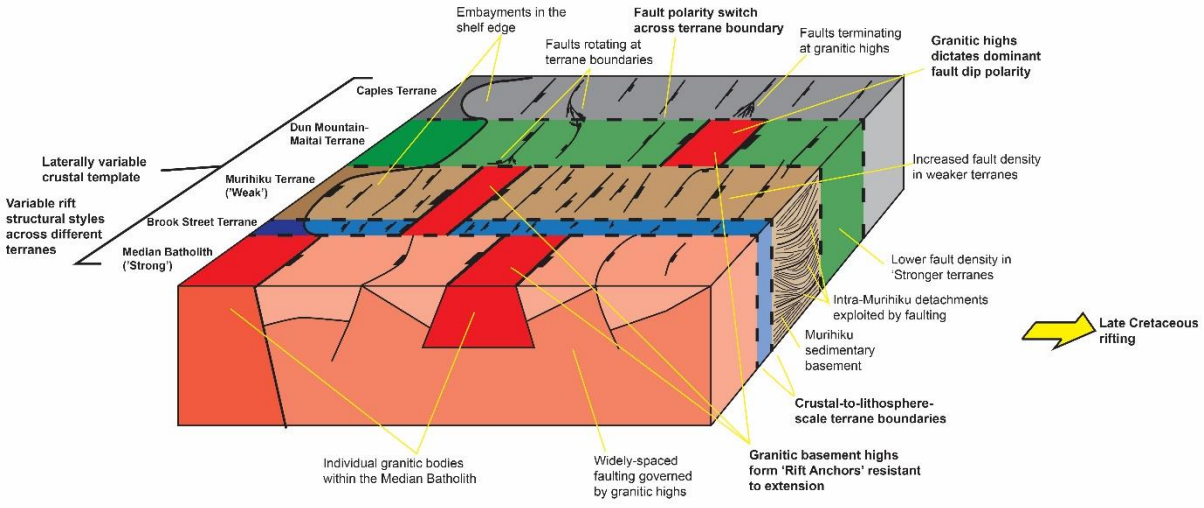

Figure 11 – Schematic diagram highlighting the structural styles of rifting present across the distinct basement terranes of varying strength, lithology and tectonic histories present beneath the Great South Basin. The influence of relatively homogeneous granitic bodies and the boundaries between different domains are also highlighted.

In this study we have documented a number of distinct structural styles across the Great South Basin, which we relate to the varying lithologies and properties of the underlying basement terranes and their respective boundaries (Figure 11). Here, we assess how this complex crustal substrate affected the evolution of the Great South Basin, compare our observations to other rift systems globally, and also attempt to examine how natural complexities may add nuance and complicate first-order effects.

7.1 Rifting within the Great South Basin

We have constrained the geometry of the basement terranes present beneath the Great South Basin. Many of the structures identified offshore can be correlated to prominent features onshore. For example, the Livingstone Fault forms the boundary between the Caples and DMM terrane (Tarling et al., 2019; Phillips and Magee, 2020), whilst the Southland Syncline can be traced in the offshore region (Tulloch et al., 2019).

We identify two embayments along the western margin of the rift, that correlate with the offshore projections of the Brook Street and DMM terranes in the south and north, respectively. The southern

embayment is also associated with a NW-dipping fault that dips towards the rift margin as opposed to dipping away as it does elsewhere (Figure 3, 6). We suggest that the southern margin embayment, and specifically these NW-dipping faults, represent the eastern continuation of the Sisters Shear Zone, located along the southern coast of Stewart Island to the west. The impingement of this shear zone, which was active during the Late Cretaceous rift phase (Kula et al., 2009), along the rift margin leads to the development of a margin embayment. This does not seem to be the case for the northern margin however, which may reflect a difference in strength between the Murihiku and DMM terranes (Figure 11).

Rift activity in the GSB has previously been proposed to relate to two events: i) the separation of Australia and Zealandia and the northwards propagation of the Tasman spreading ridge; and ii) the subsequent separation of Zealandia and Western Antarctica (Kula et al., 2009). These events may be expressed as discrete rift phases within the GSB, or a protracted, multidirectional phase (Barrier et al., 2020). The primary influence in the GSB appears to be the NW-SE-oriented rift phase associated with the separation of Zealandia and Western Antarctica, leading to the dominant NE-SW fault orientation across the basin (Figure 3), although minor NW-SE trending faults are also present (Phillips and McCaffrey, 2019; Sahoo et al., 2020).

Aside from the varying structural styles between terranes (Figure 3), which we examine in detail in the following section, we also identify a change in structural style across all terranes towards the east, where the basin is characterised by a condensed and possibly truncated post-rift interval (Figures 4-8). Based on our quantitative analyses, this condensed succession does not appear to reflect changes in the amount of extension across the rift, as would be expected for an intra-basinal high or the eastern rift margin. Thick syn-rift sequences and relatively high fault heaves are often present at depth, particularly beneath the DMM/Caples terrane (Figure 6, 8). This may indicate that after the initial phase of Late Cretaceous rifting, the area represented a relative high. Some areas may have experienced erosion whilst the majority had limited accommodation space (Figure 6). In the Caples terranes, continued uplift would be required throughout the deposition of this post-rift interval to counteract the post-rift thermal subsidence associated with the prior rift activity observed below

(Figure 7). We note that this area is also associated with a number of basement highs that appear acoustically transparent on seismic data (Figure 6, 8). Based on their acoustically transparent seismic nature, and the typical lack of extension across them, we suggest that these represent granitic bodies within various basement terranes. Isostatic effects associated with these low-density structures may account for the uplift in this area. We suggest that the locus of rifting was initially in the western part of the GSB, producing the major depocentre within the Murihiku Terrane, although activity also occurred to the east, creating the large Cretaceous depocentres (Figure 7, 8). Rifting would be localised around the margin of the granitic highs, producing the large-scale boundary faults (Figure 8). The isostatic effect associated with these granitic highs may have had a more regional influence along the eastern section of the rift, with areas of limited accommodation space continuing a short distance away from the granitic highs (Figure 7).

7.2 Characteristic structural styles across 'Strong' and 'Weak' basement

Previous studies of rift physiography in the GSB have suggested that faults are dominantly listric and sole onto a mid-crustal detachment at depth (Uruski et al., 2008). Whilst this does appear to match our observations within the DMM/Caples terranes, it does not appear to be the case elsewhere across the basin, where rift physiography is much more variable.

The various terranes that underpin the Great South Basin can be classified as relatively 'strong' or relatively 'weak'. During rifting, each of these terranes manifests strain differently, producing highly variable structural styles across the rift (Figure 11). A key first-order observations is that the top basement surface appears to be relatively shallow across the Median Batholith compared to the other terranes (Figure 2, 3, 4). One possibility is that the Median Batholith experienced less extension than the other terranes and thus remained shallow as less faulting developed. This is in agreement with the lower calculated beta factor across the Median Batholith (~1.1) compared to the other terranes (~1.5/1.6), which indicated less major faulting occurred across the Median Batholith. The dominantly granitic nature of the Median Batholith suggest that it would form a relatively strong area and may resist extension, similar to other examples, including: i) the granite-cored Utsira High in the North

Sea, which initially resisted and then buffered extension throughout multiple rift events (Phillips et al., 2019); ii) the Sierra Nevada Batholith in the USA, which acts as a buffer and backstop to extension in the Basin and Range province (Ryan et al., 2020); iii) the Cornubian Batholith, which buffers multiple phases of extension (Shail and Leveridge, 2009); and iv) the cratonic Bangwelu Block of the Lake Tanganyika rift, East Africa, where strain localisation is inhibited (Wright et al., 2020). Observations from analog modelling (Beniest et al., 2018; Samsu et al., 2021) and numerical modelling (Phillips et al., 2022) demonstrate that strain will preferentially localise in relatively weaker areas whilst strong areas resist strain localisation.

We suggest a relative absence of heterogeneities within the Median Batholith result in a lack of areas for strain to localise during rifting, accounting for its apparent strength. Nevertheless, the Median Batholith also contains a prominent basement fabric, which we interpret to represent pervasive sub-seismic faulting that reflects the absence of larger faults where strain has localised. Deformation within the Median Batholith is therefore largely characterised by small-scale faulting, with little strain localisation occurring (Figure 4, 11). Whilst heterogeneities are not pervasive throughout the Median Batholith compared to the adjacent terranes some weaknesses may still be present. For example, the boundaries between pluton suites may represent weaknesses that can inhibit fault propagation or cause strain to localise (Muir et al., 2000; Allibone and Tulloch, 2004; Phillips and McCaffrey, 2019). We suggest that the large, basement high-bounding faults exploited any weaknesses that may have been present within the batholith (Figure 11). Based on this interpretation, and given that the terranes are oriented parallel to the regional stress field such that all terranes are subject to the same regional stress, we suggest that the Median Batholith experienced roughly the same degree of extension as other terranes. Within the Median Batholith, this strain was mostly accommodated by smaller, potentially sub-seismic, scale faulting that are not incorporated into our transect analyses. We suggest that the overall shallower nature of the top basement surface across the Median Batholith reflects the fact that these low-displacement faults do not produce major depocentres and extension is more akin to uniform thinning, similar to numerical modelling observations of Phillips et al., (2023). The

shallow Median Batholith may also reflect the relatively low density and buoyant nature of the dominantly granitic batholith (Howell et al., 2019).

In contrast to the Median Batholith, the predominantly sedimentary Murihiku Terrane may be classed as relatively weak (Figure 11). The largest depocentre across the GSB is situated atop the Murihiku Terrane, suggesting large amounts of extension, this is corroborated by the large beta-factors measured across the transects (1.5-1.6) (Figure 6). The pre-existing faults, along with the sedimentary layering within Murihiku Terrane basement may represent potential weaknesses that could be exploited during later tectonic events (Figure 11). The folding of the sedimentary layering ensures that the bedding displays a range of optimal and non-optimal orientations that could be exploited. The sedimentary layering within the Murihiku basement appears to form a prominent detachment surface for fault systems in the northern section of the terrane (Figure 5, 11). Similarly, fault systems in the south of the terrane appear to be formed of multiple segments that may similarly exploit detachments, although the detachments are not resolved on the seismic reflection data (Figure 7).

We are unable to comment specifically on the apparent strength of the other terranes beneath the GSB, although we suggest that they likely fall somewhere between the Median Batholith and Murihiku terranes described above. The DMM terrane contains both a sedimentary and ophiolitic interval, and therefore may display variable properties. One key factor in determining the relative strength of these terranes however may be their width. Once faults are established they form weaknesses that can continue to localise strain. As faults are suggested to nucleate at the terrane boundaries (Sahoo et al., 2020), faults may rapidly propagate and traverse the narrow Brook Street and DMM terranes, thereby partitioning the terrane and negating its inherent strength (Phillips et al., 2023).

7.3 The influence of terrane boundaries on rift physiography

Aside from the inherent strength and internal properties of the basement terranes, the boundaries between them exert a strong influence over rift physiography (Figure 11). Sahoo et al., (2020) propose that faulting initiates at terrane boundaries in the GSB, particularly the boundary between the Murihiku and Brook Street terranes and the boundaries of the DMM terrane. The narrow nature of the

DMM terrane in plan-view means that it is difficult to determine whether faulting was concentrated within the terrane or at its boundaries. That faulting initiated at the terrane boundaries is in agreement with our observations of the Murihiku-DMM boundary, where throw maxima and the largest depocentres are located close to the terrane boundary (Figure 10), suggesting that the faults initiated at, or close to, the boundary before propagating away (Figure 9, 10). Similarly, observations from the North Sea show that faults often nucleate and propagate away from pre-existing structures (Duffy et al., 2015), whilst numerical modelling observations show how faults may be seeded at the boundaries of relatively stronger areas and propagate laterally (Phillips et al., 2023).

As well as forming nucleation points for faults during the initial stages of rifting, terrane boundaries may also represent lateral barriers to those faults that laterally propagate towards them. This may be more pronounced in the relatively narrow terranes; faults that nucleate at the boundary may rapidly propagate across the full width of the terrane and be inhibited at the adjacent boundary. This may produce compartmentalised fault systems, particularly during the early stages of rifting (Sahoo et al., 2020). Faults that nucleate at the boundaries preferentially propagate away from said boundary, producing the observed asymmetrical throw profiles, as propagation through the boundary is often inhibited (Figure 10). Faults also rotate to align with or terminate along terrane boundaries across the Great South Basin (Sahoo et al., 2020) (e.g. F5 in Figure 10, Figure 11). Strain may have accumulated along faults pinned at terrane boundaries, before they eventually propagate through (e.g. Faults 1 and 2 in Figure 10). Similar breakthrough faults are identified within the Median Batholith, where fault systems are interpreted to splay and terminating at the boundaries between individual pluton suites within the larger composite batholith, before eventually breaking through (Phillips and McCaffrey, 2019).

A key question is whether the terrane boundaries represent active (i.e. a structure that is itself a heterogeneity or weakness) or passive (i.e. the transition between terranes with differing properties and structural styles) features. The WNW-trending Terrane boundary fault between the southern margin of the Median Batholith and Western Province terranes forms an active structure as described in Phillips and McCaffrey (2019). Similarly, the Livingstone Fault between the DMM and Caples

terranes also represents an example of an active structure, forming a prominent crustal-to-lithospheric scale shear zone (Tarling et al., 2019). Observations from the North Sea have shown that pre-existing shear zones oriented at high angles to the rift may partition deformation and segment the rift (Fossen et al., 2016; Phillips et al., 2019).

In contrast, passive boundaries represent changes in the properties of basement terranes, and therefore rift structural style, with the boundary itself not necessarily representing with a specific heterogeneity or weakness. Examples may include the Turkana depression in the East African Rift, where the structural style changes from a narrow rift in the north and south, to a wide area of distributed deformation across an area of thinned lithosphere associated with earlier extension (Brune et al., 2017), or the Lake Tanganyika rift, where the transition from cratonic to orogenic belt crust corresponds to a transition from non-localised to localised faulting (Wright et al., 2020). We suggest that the boundary between the Murihiku and DMM terrane presented here represents a passive structure, accommodating thin-skinned NW-dipping faults of the Murihiku terrane in the south-east and compartmentalising them from the thick-skinned faults of the DMM/Caples terranes.

7.4 Local complexities within natural rift systems

At the whole rift-scale, we document characteristic structural styles associated with strong and weak basement terranes; stronger areas are associated with a lack of strain localisation and relatively sparse highs, whereas weaker areas are characterised by more localised, regularly-spaced fault systems (Figure 11). This is generally in agreement with observations from numerical and analog modelling (Beniest et al., 2018; Samsu et al., 2021; Phillips et al., 2023). In addition, observations from the eastern North American margin show that stronger areas resist extension, with strain localised into adjacent, relatively weaker, areas, until added impetus and thermal inputs from magmatism enable extension in the stronger areas (Lang et al., 2020).

However, at the more detailed scale, we recognise additional features that complicate the idea of ‘strong’ vs ‘weak’ areas and are often not considered or incorporated into more regional, large-scale studies. Overall, the ‘strong’ Median Batholith is characterised by a relative lack of localisation.

However, rather than being a homogeneous block, the Median Batholith represents a composite structure stitched together from individual pluton suites (Allibone and Tulloch, 2004; Muir et al., 2000; Phillips and McCaffrey, 2019; Tulloch et al., 2019). A prominent example is the Separation Point batholith suite, which occupies a position along the margin of the Median Batholith (Muir et al., 2000; Allibone and Tulloch, 2004); faults within the Median Batholith terminate at the internal boundary with the Separation Point suite (Phillips and McCaffrey, 2019). Although the boundaries between different plutons may correspond to relatively small changes in absolute strength between two relatively strong blocks, they may represent prominent weaknesses within an otherwise relatively homogeneous area (Figure 11). Whilst the Median Batholith may not be homogeneous at this scale, the constituent plutons may be relatively more homogeneous. Therefore, we suggest that any weaknesses between them would rapidly localise strain during extension. This may explain the presence of the observed rare high-displacement faults across the Median Batholith. These faults bound basement highs and may correspond to the boundaries between individual pluton suites.

Our observations suggest that faults within the DMM terrane are inhibited at the boundary with the Murihiku terrane to the south (Figure 9). This would suggest that the Murihiku terrane represents a relatively strong area, in contrast to our inferences based on extension estimates and the large depocentres present atop the terrane (Figure 5, 6). In the Murihiku Terrane, faults exploit intra-Murihiku detachments that are not present to the north and form a thin-skinned, self-contained fault system (Figure 9). Whilst the Murihiku terrane may be considered weaker than the adjacent DMM and Caples terranes, this self-contained, thin-skinned fault system forms an area of apparent strength inhibiting faults in adjacent areas from propagating into the Murihiku terrane and causing them to instead rotate along the boundary.

We identify first-order differences in the structural style and rift-physiography of the Great South Basin, which we relate to differences in the lithology and rheology of the basement terranes beneath the rift. We relate these different structural styles to relatively ‘strong’ or relatively ‘weak’ basement terranes and establish characteristic features associated with each, in agreement with regional and modelling-based studies. However, we also have also shown that there are some local features that

complicate these first-order observations when examined in more detail. Our multi-scale observations demonstrate that whilst the Median Batholith represents a strong area, there are also weaknesses within it that may be exploited by faults. Similarly, the weak 'Murihiku' terrane contains some relatively stronger areas, such as self-contained fault systems, or relatively isolated, potentially granitic-cored bodies that form basement highs. These domain-specific complexities become important when assessing natural hazard or resource implications in rift systems as these will be local features that are not necessarily predicted by numerical models or likely to emerge during regional studies. We recommend a multi-scale approach to the study of rift basins where departures from expected patterns are examined in detail to uncover domain-specific complexities that would require further in-depth investigation.

Conclusions

In this study we examine how variations in upper crustal lithology and rheology influence the geometry and evolution of rift systems, focussing on the Great South Basin, New Zealand. We characterise the structural style and evolution of the rift within distinct basement terranes. In addition, we examine the influence of isolated and homogeneous granitic bodies as well as the boundaries between different upper crustal volumes.

We extend the boundaries of basement terranes offshore beneath the Great South Basin and identify characteristic rift structural styles associated with each terrane. The dominantly granitic Median Batholith is characterised by a few large-scale faults bounding isolated highs and a lack of clear reflectivity within basement, representing a relatively strong basement terrane. In contrast, the dominantly sedimentary Murihiku Terrane represents a relatively weak basement terrane and is easily identifiable by its characteristic layered basement reflectivity. The rift in this area is characterised by large-scale faults that form part of a linked system in map-view. We suggest that these faults exploit internal weaknesses and the sedimentary layering within the Murihiku Terrane. The Caples and Dun-Mountain-Maitai terranes form a middle ground between the Median Batholith and Murihiku terranes

and is characterised by high displacement faults that appear to link at depth and sole onto a middle-crustal detachment. Quantitative analyses of the fault systems in each of these domains show the largest beta factor in the Caples and Dun Mountain-Maitai terranes, with the lowest in the Median Batholith. We suggest that extension in the Median Batholith is characterised by low-displacement structures as strain is unable to localise. Where weaknesses exist within the Median Batholith, such as at the boundaries between different plutonic suites, strain may localise producing sparsely-spaced high-displacement faults. Similarly, faulting within the Murihiku Terrane may exploit abundant weaknesses within the sedimentary basement.

Isolated granitic bodies are present across multiple terranes. These bodies are generally resistant to extension and produce basement highs that act as rift anchors and segment sections of the rift. We find that terrane boundaries segment the rift system, separating distinct sections of the rift. Faults are inhibited at the boundaries between domains and at the isolated granitic bodies. Specific heterogeneities and weaknesses within distinct basement terranes produce local complexities within the rift. For example, the presence of abundant heterogeneities within the Murihiku terrane create a localised, relatively thin-skinned fault system that is anchored by a granitic basement high. To the north, the relative lack of heterogeneities in the Dun Mountain-Maitai terrane forms a barrier to this localised fault system, with faults terminating and changing polarity across the terrane boundary. These localised features are rarely captured in numerical modelling and analog studies, which typically focus on large-scale, first-order features. This study highlights characteristic structural styles associated with areas of relatively strong and weak areas of crust characterised by differing and varied structures. These distinct basement terranes and the presence of the localised and varied heterogeneities within them produces a rift that reflects the highly complex crustal substrate. Understanding how this substrate influences the subsequent rift evolution becomes important for identifying domain-specific complexities, (e.g. depocentres, localised fault systems, strain shadows) that are important for natural hazard or resource evaluation in these systems.

Data availability

Seismic reflection and well data used in this study are publically available online via the New Zealand Petroleum and Minerals Exploration Database (https://www.nzpam.govt.nz/maps-geoscience/exploration-database/).

References

Allibone, A. H., & Tulloch, A. J. (2004). Geology of the plutonic basement rocks of Stewart Island, New Zealand. New Zealand Journal of Geology and Geophysics, 47(2), 233-256.

Bache, F., Sutherland, R., Stagpoole, V., Herzer, R., Collot, J., & Rouillard, P. (2012). Stratigraphy of the southern Norfolk Ridge and the Reinga Basin: A record of initiation of Tonga–Kermadec–Northland subduction in the southwest Pacific. Earth and Planetary Science Letters, 321, 41-53.

Barrier, A., Nicol, A., Browne, G. H., & Bassett, K. N. (2020). Late Cretaceous coeval multi-directional extension in South Zealandia: Implications for eastern Gondwana breakup. Marine and Petroleum Geology, 118, 104383.

Beggs, J. M. (1993). Depositional and tectonic history of the Great South Basin. In South Pacific sedimentary basins (Vol. 2, pp. 365-373). Elsevier Amsterdam.

Beniest, A., Willingshofer, E., Sokoutis, D., & Sassi, W. (2018). Extending continental lithosphere with lateral strength variations: effects on deformation localization and margin geometries. Frontiers in Earth Science, 6, 148.

Bishop, D. G., Bradshaw, J. D., Landis, C. A., & Turnbull, I. M. (1976). Lithostratigraphy and structure of the Caples terrane of the Humboldt Mountains, New Zealand. New Zealand journal of geology and geophysics, 19(6), 827-848.

Bishop, D. G., Bradshaw, J. D., & Landis, C. A. (1985). Provisional terrane map of South Island, New Zealand.

Bradshaw, J. D. (1989). Cretaceous geotectonic patterns in the New Zealand region. Tectonics, 8(4), 803-820.

Cooper, A. F., Barreiro, B. A., Kimbrough, D. L., & Mattinson, J. M. (1987). Lamprophyre dike intrusion and the age of the Alpine Fault, New Zealand. Geology, 15, 941– 944. http://doi.org/10.1130/0091-7613(1987)15<941:LDIATA>2.0.CO;2

Doré, A. G., Lundin, E. R., Fichler, C., & Olesen, O. (1997). Patterns of basement structure and reactivation along the NE Atlantic margin. Journal of the Geological Society, 154(1), 85-92.

Fulthorpe, C. S., Carter, R. M., Miller, K. G., & Wilson, J. (1996). Marshall Paraconformity: a mid-Oligocene record of inception of the Antarctic circumpolar current and coeval glacio-eustatic lowstand?. Marine and petroleum geology, 13(1), 61-77.

Grobys, J. W. G., Gohl, K., Davy, B., Uenzelmann-Neben, G., Deen, T., & Barker, D. (2007). Is the Bounty Trough off eastern New Zealand an aborted rift?. Journal of Geophysical Research: Solid Earth, 112(B3).

Grobys, J. W. G., Gohl, K., Uenzelmann-Neben, G., Davy, B., & Barker, D. (2009). Extensional and magmatic nature of the Campbell Plateau and Great South Basin from deep crustal studies. Tectonophysics, 472(1-4), 213-225.

Heilman, E., Kolawole, F., Atekwana, E. A., & Mayle, M. (2019). Controls of basement fabric on the linkage of rift segments. Tectonics, 38(4), 1337-1366.

Henza, A. A., Withjack, M. O., & Schlische, R. W. (2011). How do the properties of a pre-existing normal-fault population influence fault development during a subsequent phase of extension?. Journal of Structural Geology, 33(9), 1312-1324.

Howell, L., Egan, S., Leslie, G., Clarke, S., Mitten, A., & Pringle, J. (2020). The influence of low-density granite bodies on extensional basins. Geology Today, 36(1), 22-26.

Jugum, D., Stewart, E., Palin, J. M., Mortimer, N., Norris, R. J., & Lamb, W. M. (2019). Correlations between a heterogeneous mantle and multiple stages of crustal growth: a review of the Dun Mountain ophiolite, New Zealand. Geological Society, London, Memoirs, 49(1), 75-92.

Kamp, P. J., & Liddell, I. J. (2000). Thermochronology of northern Murihiku Terrane, New Zealand, derived from apatite FT analysis. Journal of the Geological Society, 157(2), 345-354.

Kimbrough, D. L., Mattinson, J. M., Coombs, D. S., Landis, C. A., & Johnston, M. R. (1992). Uranium-lead ages from the Dun Mountain ophiolite belt and Brook Street terrane, South Island, New Zealand. Geological Society of America Bulletin, 104(4), 429-443.

Kula, J., Tulloch, A., Spell, T. L., & Wells, M. L. (2007). Two-stage rifting of Zealandia-Australia-Antarctica: evidence from 40Ar/39Ar thermochronometry of the Sisters shear zone, Stewart Island, New Zealand. Geology, 35(5), 411-414.

Kula, J., Tulloch, A. J., Spell, T. L., Wells, M. L., & Zanetti, K. A. (2009). Thermal evolution of the Sisters shear zone, southern New Zealand; Formation of the Great South Basin and onset of Pacific-Antarctic spreading. Tectonics, 28(5).

Lang, G., ten Brink, U. S., Hutchinson, D. R., Mountain, G. S., & Schattner, U. (2020). The Role of Premagmatic Rifting in Shaping a Volcanic Continental Margin: An Example From the Eastern North American Margin. Journal of Geophysical Research: Solid Earth, 125(11), e2020JB019576.

Lever, H. (2007). Review of unconformities in the late Eocene to early Miocene successions of the South Island, New Zealand: ages, correlations, and causes. New Zealand Journal of Geology and Geophysics, 50(3), 245-261.

Mair, J. A., & Green, A. G. (1981). High-resolution seismic reflection profiles reveal fracture zones within a ‘homogeneous’ granite batholith. Nature, 294(5840), 439-442.

McWilliams, M. O., & Howell, D. G. (1982). Exotic terranes of western California. Nature, 297(5863), 215-217.

Mortimer, N. (2004). New Zealand's geological foundations. Gondwana research, 7(1), 261-272.

Mortimer, N., Davey, F. J., Melhuish, A., Yu, J., & Godfrey, N. J. (2002). Geological interpretation of a deep seismic reflection profile across the Eastern Province and Median Batholith, New Zealand: crustal architecture of an extended Phanerozoic convergent orogen. New Zealand Journal of Geology and Geophysics, 45(3), 349-363.

Mortimer, N., Rattenbury, M. S., King, P. R., Bland, K. J., Barrell, D. J. A., Bache, F., ... & Turnbull, R. E. (2014). High-level stratigraphic scheme for New Zealand rocks. New Zealand Journal of Geology and Geophysics, 57(4), 402-419.

Mortimer, N., Tulloch, A. J., Spark, R. N., Walker, N. W., Ladley, E., Allibone, A., & Kimbrough, D. L. (1999). Overview of the Median Batholith, New Zealand: a new interpretation of the geology of the Median Tectonic Zone and adjacent rocks. Journal of African earth sciences, 29(1), 257-268.

Moy, D. J., & Imber, J. (2009). A critical analysis of the structure and tectonic significance of rift-oblique lineaments (‘transfer zones') in the Mesozoic–Cenozoic succession of the Faroe–Shetland Basin, NE Atlantic margin. Journal of the Geological Society, 166(5), 831-844.

Muir, R. J., Bradshaw, J. D., Weaver, S. D., & Laird, M. G. (2000). The influence of basement structure on the evolution of the Taranaki Basin, New Zealand. Journal of the Geological Society, 157(6), 1179-1185.

Pascal, C., Van Wijk, J. W., Cloetingh, S. A. P. L., & Davies, G. R. (2002). Effect of lithosphere thickness heterogeneities in controlling rift localization: numerical modeling of the Oslo Graben. Geophysical Research Letters, 29(9), 69-1.

Philippon, M., Willingshofer, E., Sokoutis, D., Corti, G., Sani, F., Bonini, M., & Cloetingh, S. (2015). Slip re-orientation in oblique rifts. Geology, 43(2), 147-150.

Phillips, T. B., Jackson, C. A., Bell, R. E., Duffy, O. B., & Fossen, H. (2016). Reactivation of intrabasement structures during rifting: A case study from offshore southern Norway. Journal of Structural Geology, 91, 54-73.

Phillips, T. B., & Magee, C. (2020). Structural controls on the location, geometry and longevity of an intraplate volcanic system: the Tuatara Volcanic Field, Great South Basin, New Zealand. Journal of the Geological Society, 177(5), 1039-1056.

Phillips, T. B., & McCaffrey, K. J. (2019). Terrane Boundary Reactivation, Barriers to Lateral Fault Propagation and Reactivated Fabrics: Rifting Across the Median Batholith Zone, Great South Basin, New Zealand. Tectonics, 38(11), 4027-4053.

Phillips, T., Naliboff, J., McCaffrey, K., Pan, S., van Hunen, J., & Froemchen, M. (2022). The influence of crustal strength on rift geometry and development–Insights from 3D numerical modelling. EGUsphere, 1-29.

Robertson, A. H., & Palamakumbura, R. (2019). Geological development and regional significance of an oceanic magmatic arc and its sedimentary cover: Permian Brook Street Terrane, South Island, New Zealand. Geological Society, London, Memoirs, 49(1), 43-73.

Rotevatn, A., Kristensen, T. B., Ksienzyk, A. K., Wemmer, K., Henstra, G. A., Midtkandal, I., ... & Andresen, A. (2018). Structural inheritance and rapid rift-length establishment in a multiphase rift: The East Greenland rift system and its Caledonian orogenic ancestry. Tectonics, 37(6), 1858-1875.

Ryan, J., Frassetto, A. M., Hurd, O., Jones, C. H., Unruh, J., Zandt, G., ... & Owens, T. J. (2020). Unusually deep earthquakes in the central Sierra Nevada (California, USA): Foundering ultramafic lithosphere?. Geosphere, 16(1), 357-377.

Sahoo, T., King, P., Bland, K., Strogen, D., Sykes, R., & Bache, F. (2014). Tectono-sedimentary evolution and source rock distribution of the mid to Late Cretaceous succession in the Great South Basin, New Zealand. The APPEA Journal, 54(1), 259-274.

Sahoo, T. R., Nicol, A., Browne, G. H., & Strogen, D. P. (2020). Evolution of a normal fault system along eastern Gondwana, New Zealand. Tectonics, 39(10), e2020TC006181.

Samsu, A., Cruden, A. R., Molnar, N. E., & Weinberg, R. F. (2021). Inheritance of penetrative basement anisotropies by extension-oblique faults: Insights from analogue experiments. Tectonics, e2020TC006596.

Samsu, A., Micklethwaite, S., Williams, J., Fagereng, A., & Cruden, A. R. (2022). A review of structural inheritance in rift basin formation.

Shail, R. K., & Leveridge, B. E. (2009). The Rhenohercynian passive margin of SW England: Development, inversion and extensional reactivation. Comptes Rendus Geoscience, 341(2-3), 140-155. https://doi.org/10.1016/j.crte.2008.11.002

Spandler, C., Worden, K., Arculus, R., & Eggins, S. (2005). Igneous rocks of the Brook Street Terrane, New Zealand: Implications for Permian tectonics of eastern Gondwana and magma genesis in modern intra-oceanic volcanic arcs. New Zealand Journal of Geology and Geophysics, 48(1), 167-183.

Sutherland, R., Collot, J., Lafoy, Y., Logan, G. A., Hackney, R., Stagpoole, V., Uruski, C., Hashimoto, T. (2010). Lithosphere delamination with foundering of lower crust and mantle caused permanent subsidence of New Caledonia trough and transient uplift of Lord Howe Rise during Eocene and Oligocene initiation of Tonga-Kermadec subduction, western Pacific. Tectonics, 29, TC2004. http://doi.org/10.1029/2009TC002476

Sutherland, R., Davey, F., & Beavan, J. (2000). Plate boundary deformation in South Island, New Zealand, is related to inherited lithospheric structure. Earth and Planetary Science Letters, 177, 141–151. http://doi.org/https://doi.org/10.1016/S0012-821X(00)00043-1

Thomas, W. A. (2006). Tectonic inheritance at a continental margin. GSA today, 16(2), 4-11.

Tulloch, A. J., Mortimer, N., Ireland, T. R., Waight, T. E., Maas, R., Palin, J. M., ... & Turnbull, R. E. (2019). Reconnaissance basement geology and tectonics of South Zealandia. Tectonics, 38(2), 516-551.

Uruski, C. I. (2010). New Zealand's deepwater frontier. Marine and Petroleum Geology, 27(9), 2005-2026.

Vasconcelos, D. L., Bezerra, F. H., Clausen, O. R., Medeiros, W. E., de Castro, D. L., Vital, H., & Barbosa, J. A. (2019). Influence of Precambrian shear zones on the formation of oceanic fracture zones along the continental margin of Brazil. Marine and Petroleum Geology, 101, 322-333.

Whipp, P. S., Jackson, C. L., Gawthorpe, R. L., Dreyer, T., & Quinn, D. (2014). Normal fault array evolution above a reactivated rift fabric; a subsurface example from the northern Horda Platform, Norwegian North Sea. Basin Research, 26(4), 523-549.

Wilson, J. T. (1966). Did the Atlantic close and then re-open?.